Quantitative Theory for the Growth Rate and Amplitude of the Compressible Richtmyer-Meshkov Instability at all Density Ratios

Qiang Zhang,[1] Shuyan Deng,[2] and Wenxuan Guo[1]

[1]*Department of Mathematics, City University of Hong Kong, 83 Tat Chee Avenue, Kowloon 999077, Hong Kong*
[2]*Institute of Architecture and Civil Engineering, Guangdong University of Petrochemical Technology,*
139 Guanduerlu Road, Maoming, Guangdong 525000, China

Theoretical treatment of the Richtmyer-Meshkov instability in compressible fluids is a challenging task due to the presence of compressibility and nonlinearity. In this Letter, we present a quantitative theory for the growth rate and the amplitude of fingers in Richtmyer-Meshkov instability for compressible fluids based on the methods of the two-point Padé approximation and asymptotic matching. Our theory covers the entire time domain from early to late times and is applicable to systems with arbitrary fluid density ratios. The theoretical predictions are in good agreement with data from several independent numerical simulation methods and experiments.

When a shock hits a material interface between two compressible fluids of different densities, unstable bubbles (light fluids penetrating into heavy ones) and spikes (heavy fluids penetrating into light ones) develop. This is known as the Richtmyer-Meshkov instability (RMI) [1,2] and is important for science and technology, such as supernova and inertial confinement fusion. Extensive works on the RMI can be traced from Refs. [1–20] and from recent review papers [21,22]. We consider two compressible inviscid fluids in a vertically infinite strip with its left and right boundaries satisfying periodic conditions. The initial material interface contains a single-mode sinusoidal perturbation. An important issue of the RMI is how the amplitude of the unstable interface grows. We present an analytic theory for the growth rates and amplitudes of compressible RMI. Our theory is applicable to systems with arbitrary density ratios and is valid for all times. Compressibility and nonlinearity make the theoretical treatment extremely challenging. There are sets of experimental data [3,4] and numerical data [5,6] available for compressible RMI. However, there is still a lack of accurate theoretical predictions for finger development in compressible fluids for all times. Here we present such a theory. Our predictions are in good agreement with numerical and experimental data from early to late times, even for a Mach 15.3 incident shock.

Richtmyer predicted this instability and developed a linear theory for compressible fluids in the case of reflected shocks [1]. Meshkov confirmed this experimentally [2]. The linear theory of compressible RMI was further studied in Ref. [7] for reflected shock cases and was extended to reflected rarefaction wave cases in Ref. [8]. A nonlinear theory for compressible RMI can be found in Refs. [9,10]. For incompressible RMI with an infinite density ratio, Hecht,

Alon, and Shvarts [11] applied a Layzer-type approximation [12] to bubbles. This approach was extended by Mikaelian for bubbles [13,14] and by Zhang for spikes [15]. For incompressible RMI with a finite density ratio, theoretical approaches were carried out by Goncharov [16], Abarzhi, Glimm, and Lin [17], and Sohn [18]. It was pointed out that Goncharov's approach [16] led to several incorrect results [19]. In particular, it gives wrong predictions for spikes. Recently, a new model without these shortcomings has been developed to predict the growth rates of bubbles and spikes at all density ratios [20].

We use a signed Atwood number $A = (\rho' - \rho)/(\rho' + \rho)$, where ρ and ρ' are the densities of two fluids. $A > 0$ is for bubbles, and $A < 0$ is for spikes. This allows the same functional form for bubbles and spikes. The propagation direction of the incident shock affects the reflected wave type but not the sign of A, which depends only on the finger type.

Our purpose is to develop a theory which can provide accurate predictions for growth rates and amplitudes of fingers in compressible fluids for arbitrary Atwood numbers and over all times. We also require that our theory satisfy all known properties. For compressible fluids:

(i) for a small initial perturbation amplitude, the growth rate of a finger at early times is governed by the compressible linear theory $v_{\text{lin}}^{\text{cmp}}(t, A)$ [1,7,8].

For incompressible fluids:

(ii) for early times, the growth rate of a finger is [10]

$$v = v_0 - kv_0^2(A + ka_0)t + k^2 v_0^3 \left(A^2 - \frac{1}{2} + 2Aka_0\right)t^2$$

$$+ \frac{4}{3}k^3 v_0^4(A - A^3)t^3 + O(t^4); \tag{1}$$

(iii) for $A = 1$, the bubble growth rate tends to zero [11,15,18];

(iv) for $A = -1$, the spike growth rate tends to a constant $v_0[(3 + 3ka_0)/(1 + 3ka_0)]^{1/2}$ [15];

(v) for arbitrary A, the asymptotic growth rate of a finger (bubble or spike) is $v_{\text{asym}} \sim [1/\alpha(A)kt]$ with $\alpha(A) = \frac{3}{4}\{[(1 + A)(3 + A)]/[3 + A + \sqrt{2}(1 + A)^{1/2}]\}\{[4(3 + A) + (9 + A) \times \sqrt{2}(1 + A)^{1/2}]/[(3 + A)^2 + 2(3 - A)\sqrt{2}(1 + A)^{1/2}]\}$ [20].

In properties (ii)–(v), $A > 0$ is for bubbles and $A < 0$ is for spikes, a_0 is the initial perturbation amplitude, k is the wave number, and v_0 is the initial growth rate.

Since the RMI is induced by an incident shock, one naturally needs to consider the compressibility of fluids. Furthermore, the finger development at unstable interfaces is nonlinear. Therefore, compressibility and nonlinearity are two major obstacles to developing an accurate quantitative theory for compressible RMI. We develop such a theory based on the following physical picture. By definition, compressibility measures the changes in density resulting from changes in pressure. For the RMI, the large changes in pressure occur in the vicinity of shocks. At early times, the incident shock, the transmitted shock, and the reflected wave interact with the material interface, and the compressibility effects are important. Thus, for an RM interface with a small initial perturbation, the dynamics is governed by the compressible linear theory [1,7,8]. However, after the transmitted shock and the reflected wave have propagated away from the material interface, there are no large changes in pressure in the vicinity of fingers. Thus, the compressibility effects become less important. This is because, although the fluids are compressible, the system does not provide an environment to reveal the compressibility. The compressibility effects are progressively decreasing with time, and the nonlinearity effects are progressively increasing. Thus, the system gradually changes from a linear and compressible stage at early times to a nonlinear and incompressible stage at late times. With this understanding, our approach consists of two steps: (i) Since the dynamics at late times is different from that at early times, we treat the former separately from the latter and develop an approximate solution for the nonlinear incompressible system using a two-point Padé approximation method. (ii) By applying an asymptotic matching technique, we match the compressible linear theory at early times and the incompressible nonlinear theory at late times to obtain an approximate solution for the compressible system at all Atwood numbers and over all times. This matching leads to compressibility dependence of the late-time solution.

Step (i).—Since the early-time compressible linear theory is known, we need only to construct an approximate solution for incompressible RMI, which offers a good approximation for compressible RMI at late times. Let $v_{\text{nl}}^{\text{incmp}}(t, A)$ be the finger growth rate at an incompressible RM interface in the nonlinear stage. We apply the Padé approximation [23], which approximates a function by a ratio of two polynomials: $P_n^m(t) = P^m(t)/P^n(t)$, where $P^m(t)$ and $P^n(t)$ are polynomials of degree m and n, respectively. This gives

$$v_{\text{nl}}^{\text{incmp}}(t, A) = v_0(A)P_3^2(t, A, v_0(A)), \qquad (2)$$

where

$$P_3^2(t, A, v_0(A)) = \frac{1 + a_1(A)[kv_0(A)]t + a_2(A)[kv_0(A)]^2t^2}{1 + b_1(A)[kv_0(A)]t + b_2(A)[kv_0(A)]^2t^2 + b_3(A)[kv_0(A)]^3t^3}. \qquad (3)$$

The dimensionless coefficients $a_i(A)$ with $i = 1$, 2, and $b_i(A)$ with $i = 1$, 2, 3, are to be determined. For conciseness, here we do not explicitly display the dependence of these coefficients on ka_0.

Properties (ii)–(v) provide us the information about the fingers' behavior at both small and large times, whereby we construct a two-point Padé approximant with

$$a_i(A) = \beta_i(A) + \gamma_i(A)b_1(A), \qquad i = 1, 2, \qquad (4)$$

$$b_i(A) = \sigma_i(A) + \omega_i(A)b_1(A), \qquad i = 2, 3, \qquad (5)$$

where

$$\beta_1(A) = -(A + ka_0), \qquad \beta_2(A) = \lambda(A)[2A^3 - 5A - (18A^2 - 3)ka_0 - 12A(ka_0)^2],$$

$$\gamma_1(A) = 1, \qquad \gamma_2(A) = \lambda(A)[3 + 6(ka_0)^2],$$

$$\sigma_2(A) = \lambda(A)[8A^3 - 6A^2\alpha(A) - 8A + 3\alpha(A) - 12A\alpha(A)ka_0], \qquad \sigma_3(A) = \alpha(A)\beta_2(A),$$

$$\omega_2(A) = \lambda(A)\{3 - 6A^2 + 6\alpha(A)A - [12A - 6\alpha(A)]ka_0\}, \qquad \omega_3(A) = \alpha(A)\gamma_2(A),$$

$$\lambda(A) = \frac{1}{6(\alpha - A - ka_0)} > 0 \quad \text{for } ka_0 < 1/2,$$

$$b_1(A) = \frac{1}{4}(c_1 + c_2)(3 - A^2)A + \frac{1}{2}(c_1 - c_2),$$

in which

$$c_1 = \frac{3}{2} \frac{(1 + 4ka_0)[(1 - 2ka_0)(2 + 4k^2a_0^2)^{1/2} - (1 + 4ka_0)ka_0]}{2 - 8ka_0 + 11(ka_0)^2 - 24(ka_0)^3},$$

$$c_2 = \frac{(1 - ka_0)(1 - 4ka_0)}{1 + (\frac{3+3ka_0}{1+3ka_0})^{1/2}(1 - 4ka_0) + 2(ka_0)^2}.$$

One can check that properties (ii)–(v) are satisfied by expanding Eq. (2) in terms of small and large t. Therefore, the two-point Padé approximant given by Eqs. (2)–(5) satisfies all known properties of incompressible RMI.

Equations (2)–(5) do not have spurious singularities: The denominator of Eq. (3) never vanishes when $ka_0 < 1/4$. When $ka_0 < 1/4$, $b_2(A)$ and $b_3(A)$ have positive minimum values at $A = -1$, and $b_1(A)$ is a nondecreasing function of A. Thus, it is sufficient to show that, at $A = -1$, the minimum value of the denominator of Eq. (3) never reaches zero for all $t \geq 0$. At $A = -1$, Eqs. (4) and (5) become, respectively,

$$a_1 = (1 - ka_0)[1 - (1 - 4ka_0)q(ka_0)],$$
$$a_2 = \frac{(1 - 4ka_0)^2}{2}\left(\frac{3 + 3ka_0}{1 + 3ka_0}\right)^{1/2}q(ka_0), \qquad (6)$$

$$b_1 = -(1 - 4ka_0)(1 - ka_0)q(ka_0),$$
$$b_2 = \frac{(1 - 4ka_0)^2}{2}q(ka_0),$$
$$b_3 = 0, \qquad (7)$$

where $q(ka_0) = \{1 + [(3+3ka_0)/(1+3ka_0)]^{1/2}(1-4ka_0) + 2(ka_0)^2\}^{-1} > 0$ for $ka_0 < 1/4$. Let $D(t)$ be the denominator of Eq. (3) at $A = -1$. We write $D(t) = 3/4 + H(t)$, where $H(t) = b_2k^2v_0^2t^2 + b_1kv_0t + 1/4$. One can show that $D(t) > 3/4$ for $ka_0 < 1/4$ from the facts that $b_2k^2v_0^2 > 0$ and the discriminant of $H(t)$ is negative. Property (iv) cannot be satisfied when $ka_0 = 1/4$, since $\lim_{t \to \infty} v_{nl}^{incmp}(t, -1) = \infty$. This proves that our Padé approximant given by Eqs. (2)–(5) is nonsingular for all $A \in [-1, 1]$ and $t \geq 0$ when $ka_0 < 1/4$.

Equation (2) is an approximate nonlinear solution for incompressible fluids. Based on the physical picture that the system gradually changes from a linear and compressible stage at early times to a nonlinear and incompressible stage at late times, Eq. (2) is also an approximate nonlinear solution for compressible fluids at late times as the compressibility effects become negligible. At early times, the solution is given by $v_{lin}^{cmp}(t, A)$, the linear theory for compressible fluids [1,7,8]. To develop a nonlinear theory for compressible fluids, we need to construct an expression which smoothly matches the compressible linear solution $v_{lin}^{cmp}(t, A)$ at early times and the incompressible nonlinear solution $v_{nl}^{incmp}(t, A)$ given by Eq. (2) at late times.

Step (ii).—To construct an approximate solution for nonlinear compressible RMI, we adopt an asymptotic matching technique developed for boundary layer problems which contain two distinct solutions for inside and outside the boundary layer, namely, the inner and outer solutions. Since we have an initial-value problem rather than a boundary-value problem, here the "inner" solution is $v_{lin}^{cmp}(t, A)$ given by the compressible linear theory, and the "outer" solution is $v_{nl}^{incmp}(t, A)$ given by Eq. (2). Analogous to the boundary layer problem, $v_0(A)$ and a_0 are the effective initial conditions of the outer solution which are different from the initial conditions of the inner solution, namely, the initial conditions of the compressible linear theory. A recipe for determining $v_0(A)$ in Eq. (2) is proposed by Prandtl: Setting the large-time limit of the inner solution and the small-time limit of the outer solution equal [24], i.e., $\lim_{t \to \infty} v_{lin}^{cmp}(t,A) = \lim_{t \to 0} v_{nl}^{incmp}(t,A)$, which leads to $v_0(A) = v_\infty(A)$. Here $v_\infty(A) \equiv v_{lin}^{cmp}(\infty, A)$ is the asymptotic growth rate in the compressible linear theory. Thus, Eq. (2) becomes

$$v_{nl}^{incmp}(t, A) = v_\infty(A)P_3^2(t, A, v_\infty(A)). \qquad (8)$$

In Eqs. (2)–(5) and (8), $A = A^+$, where A^+ is the postshock Atwood number. Matching also gives $a_0 = a_0^+$ for reflected shocks and $a_0 = \bar{a}_0 = |a_0^- + a_0^+|/2$ for reflected rarefaction waves [1,7,8], where a_0^- and a_0^+ are the pre- and postshock initial amplitudes, respectively. The absolute sign in $\bar{a}_0$ is due to the possibilities of $(a_0^- + a_0^+) < 0$ in the case of direct or indirect phase inversions. Our outer incompressible solution has a strong dependence on compressibility, since the effective initial conditions a_0 and v_0 have a strong dependence on v_∞.

Finally, we construct an expression which smoothly matches $v_{lin}^{cmp}(t, A)$ valid for early times and $v_{nl}^{incmp}(t, A)$ given by Eq. (8) valid for late times, reflecting the physical picture that the system goes through a transition from a linear and compressible stage at early times to a nonlinear and incompressible stage at late times. This transition behavior can be easily achieved by replacing the first factor $v_\infty(A)$ on the right-hand side of Eq. (8) with $v_{lin}^{cmp}(t, A)$. Therefore, we have a final expression for growth rates of fingers at compressible RM interfaces over all times and for all Atwood numbers when $ka_0 < 1/4$:

$$v_{nl}^{cmp}(t, A, v_\infty(A)) \equiv v_{lin}^{cmp}(t, A)P_3^2(t, A, v_\infty(A)), \quad (9)$$

where $P_3^2(t, A, v_\infty(A))$ is given by Eqs. (3)–(5). $A > 0$ is for bubbles and $A < 0$ is for spikes. Equation (9) satisfies all properties (i)–(v) and contains neither fitting parameters nor singularities when $ka_0 < 1/4$.

The finger amplitude at a compressible RM interface can be obtained by integrating both sides of Eq. (9):

$$a_{nl}^{cmp}(t, A) = a_0^+ + \int_0^t v_{nl}^{cmp}(t', A, v_\infty(A))dt'. \quad (10)$$

The initial condition of $a_{nl}^{cmp}(t, A)$ is a_0^+ for both reflected shock and reflected rarefaction wave cases, since it is the initial condition of the inner compressible linear solution.

The overall growth rate and the overall amplitude at a compressible RM interface are

$$\bar{v}_{nl}^{cmp}(t, A) = \frac{1}{2}[v_{lin}^{cmp}(t, A)P_3^2(t, A, v_\infty(A))$$
$$+ v_{lin}^{cmp}(t, A)P_3^2(t, -A, v_\infty(A))], \quad (11)$$

$$\bar{a}_{nl}^{cmp}(t, A) = \left| a_0^+ + \frac{1}{2}\int_0^t [v_{lin}^{cmp}(t, A)P_3^2(t, A, v_\infty(A)) \right.$$
$$\left. + v_{lin}^{cmp}(t, A)P_3^2(t, -A, v_\infty(A))]dt' \right|. \quad (12)$$

In Eqs. (11) and (12), A in $v_{lin}^{cmp}(t, A)$ and $v_\infty(A)$ does not change sign, since the results from the compressible linear theory are the same for both spikes and bubbles.

The application of the Padé approximation to the RMI was first conducted in 1997 [9,10]. However, at that time, it was possible only to construct a single-point Padé approximant based on the small-time behavior, namely, property (ii), and the result was not applicable to asymptotically large times. Since then, new information about the asymptotically large-time behavior at an arbitrary Atwood number, listed as properties (iii)–(v), has been found [11,15,18,20]. This allows us to construct a two-point Padé approximant [Eq. (9)] based on both the small- and large-time behavior, which provides predictions for growth rates and amplitudes applicable to all times. We now compare our theoretical predictions with numerical and experimental results for $ka_0 < 1/4$.

First, we consider the case that the incident shock propagates from the heavy to light fluid (from beryllium to foam). We compare our theoretical predictions of Eqs. (11) and (12) with the numerical results from Ref. [5]. Since the reflected waves are rarefaction waves, $a_0 = \bar{a}_0 = |a_0^- + a_0^+|/2$ [1,7,8]. Let s_i and M be the speed and Mach number, respectively, of the incident shock. In Figs. 1 and 2, we plot dimensionless overall growth rates $\bar{v}/s_i$ and dimensionless overall amplitudes $k\bar{a}$ as functions of dimensionless time $ks_i t$. The physical parameters of all simulations are listed in Table 2 in the Appendix of Ref. [5]. In particular, $|ka_0^-| = 0.2513$ and $A^- = 0.8681$. In Figs. 1(a) and 2(a), $M = 1.33$, $A^+ = 0.8622$, $ka_0 = 0.1883$, and
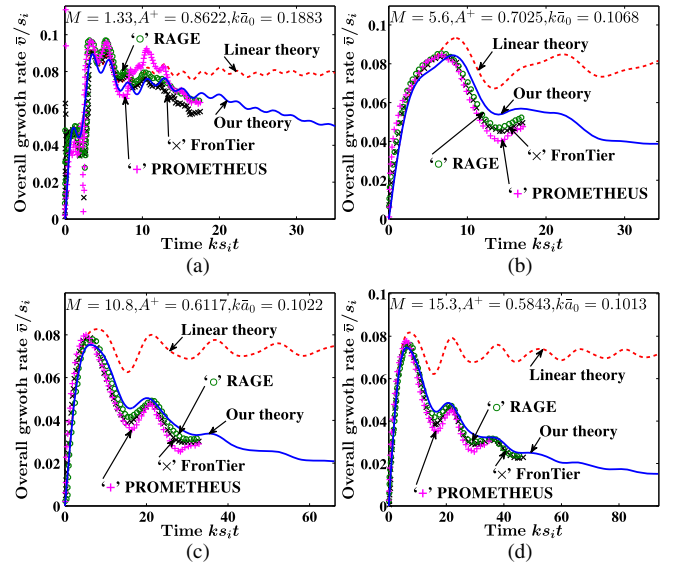
FIG. 1. Comparison for the dimensionless overall growth rates between the compressible nonlinear theory by Eq. (11) (solid line), the compressible linear theory (dashed line) [8], and three numerical simulations (× for FRONTIER, + for PROMETHEUS, and ∘ for RAGE) [5]. The parameters are in the main text.

$s_i = 4327.5$ m s^{-1}; in Figs. 1(b) and 2(b), $M = 5.6$, $A^+ = 0.7025$, $ka_0 = 0.1068$, and $s_i = 18222.2$ m s^{-1}; in Figs. 1(c) and 2(c), $M = 10.8$, $A^+ = 0.6117$, $ka_0 = 0.1022$, and $s_i = 35142.8$ m s^{-1}; in Figs. 1(d) and 2(d), $M = 15.3$, $A^+ = 0.5843$, $ka_0 = 0.1013$, and $s_i = 49785.7$ m s^{-1}. For each figure, there are three sets of numerical data obtained by
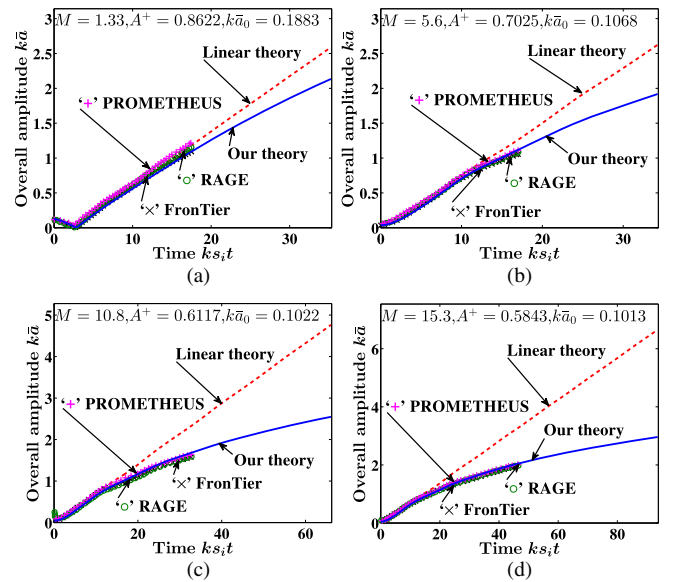
FIG. 2. Comparison for the dimensionless overall amplitudes between the compressible nonlinear theory by Eq. (12) (solid line), the compressible linear theory (dashed line) [8], and three numerical simulations (× for FRONTIER, + for PROMETHEUS, and ∘ for RAGE) [5]. The parameters are the same as those in Fig. 1.
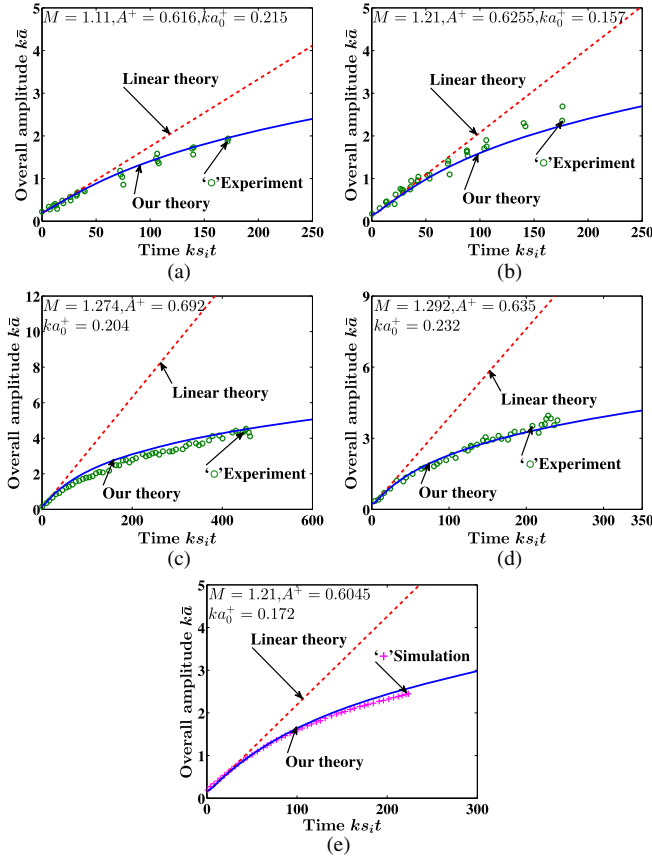
FIG. 3. Comparison for the dimensionless overall amplitudes between the compressible nonlinear theory by Eq. (12) (solid line), the compressible linear theory (dashed line) [8], the experiments (∘) [3,4], and the simulation (+) [6]. The parameters are in the main text.

three independent numerical simulations (FRONTIER [25], PROMETHEUS [26], and RAGE [27]). Figures 1 and 2 show that our theory provides excellent predictions for compressible RMI. This holds even for an incident shock with $M = 15.3$, which implies strong compressibility effects.

Second, we consider the incident shock propagating from the light to heavy fluid (from air to SF_6). The reflected waves are shocks, and thus $a_0 = a_0^+$ [1,7,8]. We compare our predictions of Eq. (12) with the experimental data in Refs. [3,4] and the numerical data in Ref. [6]. In Fig. 3, we plot $k\bar{a}$ as a function of $ks_i t$. In Figs. 3(a) and 3(b), the experimental data are from Ref. [3]. In Fig. 3(a), $M = 1.11$, $A^+ = 0.616$, $ka_0 = 0.215$, and $s_i = 312.7 \, \text{ms}^{-1}$; in Fig. 3(b), $M = 1.21$, $A^+ = 0.6255$, $ka_0 = 0.157$, and $s_i = 332.6 \, \text{m s}^{-1}$. Other parameters are listed in Table I of Ref. [3]. In Figs. 3(c) and 3(d), the experimental data are from Ref. [4]. In Fig. 3(c), $M = 1.274$, $A^+ = 0.692$, $ka_0 = 0.204$, and $s_i = 418 \, \text{m s}^{-1}$; in Fig. 3(d), $M = 1.292$, $A^+ = 0.635$, $ka_0 = 0.232$, and $s_i = 376.7 \, \text{m s}^{-1}$. Other parameters are listed in Table I of Ref. [4]. In Fig. 3(e), the numerical data are from Ref. [6]. To include

the diffusive effects at the material interface, Ref. [6] suggested that one should compare $\bar{a}_{\text{num}}(kv_0 t)$ with $\bar{a}_{\text{theory}}(kv_0 t/\psi)$. Here $\bar{a}_{\text{num}}$ and $\bar{a}_{\text{theory}}$ are the overall amplitudes from the numerical simulation and theoretical models, respectively. By rescaling the time, this is equivalent to comparing $\bar{a}_{\text{num}}(\psi ks_i t)$ with $\bar{a}_{\text{theory}}(ks_i t)$, as presented in Fig. 3(e). The parameters are $M = 1.21$, $A^+ = 0.6045$, $ka_0 = 0.172$, $s_i = 363.6 \, \text{m s}^{-1}$, and $\psi = 1.145$. Other parameters are listed in Tables I and II of Ref. [6]. Figure 3 shows that our theoretical predictions agree with the experimental and numerical data very well over the entire time period. In particular, good agreement is achieved even when $k\bar{a}$ reaches 4 [see Figs. 3(c) and 3(d)]. The significance of nonlinearity is measured by the deviation of the results from the predictions of the compressible linear theory. Except for one case [Figs. 1(a) and 2(a)], nonlinear effects are clearly shown in Figs. 1–3.

In summary, we present theoretical predictions for growth rates and amplitudes of RM unstable interfaces from early to late times for compressible fluids with arbitrary density ratios and containing no fitting parameters. It satisfies all known properties of the RMI in the literature. Our theoretical predictions are in excellent agreement with the numerical simulations and experiments for both reflected shock and reflected rarefaction wave cases. Such good agreement holds for incredibly strong shocks. It confirms that the dynamics of compressible RMI changes from linear-compressible behavior at early times to nonlinear-incompressible behavior at late times.

[1] R. D. Richtmyer, Commun. Pure Appl. Math. **13**, 297 (1960).
[2] E. E. Meshkov, Fluid Dyn. **4**, 101 (1972).
[3] B. D. Collins and J. W. Jacobs, J. Fluid Mech. **464**, 113 (2002).
[4] J. W. Jacobs and V. V. Krivets, Phys. Fluids **17**, 034105 (2005).
[5] R. L. Holmes, G. Dimonte, B. Fryxell, M. L. Gittings, J. W. Grove, M. Schneider, D. H. Sharp, A. L. Velikovich, R. P. Weaver, and Q. Zhang, J. Fluid Mech. **389**, 55 (1999).
[6] M. Latini, O. Schilling, and W. S. Don, Phys. Fluids **19**, 024104 (2007).
[7] G. Fraley, Phys. Fluids **29**, 376 (1986).
[8] Y. Yang, Q. Zhang, and D. H. Sharp, Phys. Fluids **6**, 1856 (1994).
[9] Q. Zhang and S.-I. Sohn, Phys. Lett. A **212**, 149 (1996).
[10] Q. Zhang and S.-I. Sohn, Phys. Fluids **9**, 1106 (1997).
[11] J. Hecht, U. Alon, and D. Shvarts, Phys. Fluids **6**, 4019 (1994).

[12] D. Layzer, Astrophys. J. **122**, 1 (1955).
[13] K. O. Mikaelian, Phys. Rev. Lett. **80**, 508 (1998).
[14] K. O. Mikaelian, Phys. Rev. E **67**, 026319 (2003).
[15] Q. Zhang, Phys. Rev. Lett. **81**, 3391 (1998).
[16] V. N. Goncharov, Phys. Rev. Lett. **88**, 134502 (2002).
[17] S. Abarzhi, J. Glimm, and A. Lin, Phys. Fluids **15**, 2190 (2003).
[18] S.-I. Sohn, Phys. Rev. E **67**, 026301 (2003).
[19] K. O. Mikaelian, Phys. Rev. E **78**, 015303 (2008).
[20] Q. Zhang and W. Guo, J. Fluid Mech. **786**, 47 (2016).
[21] Y. Zhou, Phys. Rep. **720-722**, 1 (2017).
[22] Y. Zhou, Phys. Rep. **723-725**, 1 (2017).
[23] A. Pozzi, *Applications of Padé Approximation Theory in Fluid Dynamics* (World Scientific, Singapore, 1994).
[24] P. A. Lagerstrom, *Matched Asymptotic Expansions* (Springer, New York, 1988).
[25] I. L. Chern, J. Glimm, O. McBryan, B. Plohr, and S. Yaniv, J. Comput. Phys. **62**, 83 (1986).
[26] B. Fryxell, E. Müller, and D. Arnett, *Hydrodynamics and Nuclear Burning* (Max-Planck-Institut für Physik und Astrophysik, Institut für Astrophysik, Garching, 1989).
[27] M. Gittings, in *Proceedings of the Defense Nuclear Agency Numerical Methods Symposium, SRI International, Palo Alto, USA* (1992).